

Sensitivity of the spherical gravitational wave detector MiniGRAIL operating at 5 K.

L. Gottardi,^{*} A. de Waard, A. Usenko, and G. Frossati

LION, Institute of Physics, Kamerlingh Onnes Laboratorium, Leiden University, Leiden, The Netherlands

M. Podt[†] and J. Flokstra

Low Temperature Division, Faculty of Science and Technology, Twente University, Enschede, The Netherlands

M. Bassan, V. Fafone, Y. Minenkov, and A. Rocchi

Dip. Fisica, Universit  Tor Vergata and INFN Roma2, Roma, Italy

(Dated: October 23, 2018)

We present the performances and the strain sensitivity of the first spherical gravitational wave detector equipped with a capacitive transducer and read out by a low noise two-stage SQUID amplifier and operated at a temperature of 5 K. We characterized the detector performance in terms of thermal and electrical noise in the system output signal. We measured a peak strain sensitivity of $1.5 \cdot 10^{-20} \text{ Hz}^{-1/2}$ at 2942.9 Hz. A strain sensitivity of better than $5 \cdot 10^{-20} \text{ Hz}^{-1/2}$ has been obtained over a bandwidth of 30 Hz. We expect an improvement of more than one order of magnitude when the detector will operate at 50 mK. Our results represent the first step towards the development of an ultracryogenic omnidirectional detector sensitive to gravitational radiation in the 3kHz range.

PACS numbers: 04.80.Nn, 95.55.Ym, 07.07.Mp, 02.60.Pn

I. INTRODUCTION

The direct observation of gravitational waves (GWs) is one of the most challenging tasks for experimental physics. After the first detection will be claimed a new branch of astronomical observation will begin and gravitational wave observatory will become more and more common facilities. A spherical detector is a perfect instrument for an astronomical observatory due to its feature of omnidirectionality and polarization sensitivity [1, 2, 3, 4, 5]. The first ultracryogenic spherical gravitational wave detectors [6, 7] are currently completing their engineering phase and will soon be operational with an expected sensitivity better than $10^{-21} \text{ Hz}^{-1/2}$ at 3 kHz . We report the results of the first sensitive measurement of the spherical gravitational wave detector Minigrail. The detector read-out is based on capacitive resonant transducers coupled to a superconducting quantum interference device (SQUID) linear amplifiers by means of superconducting transformers. The two-stage SQUID described in this work is one of the most sensitive amplifier ever used on a gravitational wave antenna. It consists on a sensor dc SQUID amplified by a Double Relaxation Oscillation Squid (DROS). The coupling of the SQUID system to the high Q electrical resonators is similar to the one developed for the AURIGA detector [8]. We obtained a coupled additive energy resolution of $700\hbar$ at 5 K in agreement with the expected values calculated

from the SQUID parameters using the standard model [9]. The spherical antenna described in this paper is the first example of a multimodal resonant detector where the five quadrupolar modes of the sphere are read-out by three resonant transducers. In this paper we discuss the noise contribution and the signal response of one read-out channel and estimate the detector sensitivity when the detector will operate at 50 mK with a complete read-out. This paper is organized as follows. In section II we described the experimental apparatus and in particular the read-out system. In section III we present and discuss the experimental results. In section III A and section III B we analyzed the electrical system, the noise spectra and equivalent temperature of the resulting coupled oscillators. Finally in section III C we describe the calibration procedure and estimate the detector strain sensitivity.

II. SYSTEM OVERVIEW

A. Sphere and mechanical transducers

MiniGRAIL is a spherical gravitational wave (GW) antenna currently under development [6]. The antenna is a massive sphere in CuAl , has a diameter of 68 cm , a mass of about 1.3 ton and the GW sensitive spheroidal quadrupole modes have frequencies around 2980 Hz at 4.2 K . The alloy CuAl6\% has been chosen because of the high quality factor ($Q \sim 10^7$ at low temperature), high sound velocity ($V_S \simeq 4100 \text{ m/s}$) and a sufficient thermal conductivity, which allows to cool a 1.3 ton antenna to a temperature below 100 mK [10]. The ultimate goal is to operate MiniGRAIL at a thermodynamic temperature of 20 mK , equipped with six transducers coupled to

^{*}Current address: SRON, National Institute for Space Research, High Energy Astrophysics Division, Utrecht, the Netherlands; Electronic address: l.gottardi@sron.nl

[†]Current address: Thales Nederland B.V., Hengelo, the Netherlands.

nearly quantum limited double-stage SQUID amplifiers [8, 11, 12]. The sphere is suspended from the centre with a gold-plated copper rod 20 mm in diameter. The rod is connected to the last mass of the mechanical vibration isolation system which consists of seven mass-spring stages suspended with stainless steel cables from three absorbers, each consisting of a stack of rubber and aluminium plates. A detailed description of the detector mechanics and cryogenics can be found in [13]

We used capacitive transducers to read-out the spheroidal modes. They consist of a closed membrane with a load mass in the centre. The electrode is made of a thin CuAl plate placed in front of the resonating mass. To obtain a small gap between resonator and electrode, we proceeded as follows. The resonator and the electrode are lapped and polished to get a smooth flat surface. Further a clean Kapton foil of a thickness equal to the desired gap is placed between the electrode and the mass. Finally a small amount of glue is added between the electrode and the support springs. A load is applied on top of the electrode in order to make a compact assembly. After the drying period of the glue the Kapton foil is removed. This technique was shown to be reliable and reproducible. Gaps of the order of $20\mu m$ could be obtained and voltage bias as large as 500 Volt could be applied without discharging.

In table I we summarise the features of the three transducers. Each resonator has an effective resonant mass of about 200 g and is tuned mainly to three different spherical modes.

Closed membrane transducers			
	transducer 1	transducer 2	transducer 3
$mass [Kg]$	0.205	0.153	0.150
$C_t [nF]$	1.17 ± 0.01	0.70 ± 0.02	1.20 ± 0.01
$gap [\mu m]$	20 ± 2	35 ± 4	25 ± 2
$f_{res} [Hz]$	2863 ± 5	2850 ± 5	2878 ± 5
Q at 300 K	$1.0 \cdot 10^4$	$1.1 \cdot 10^4$	$1.0 \cdot 10^4$
Q at 77 K	$3 \cdot 10^4$	$4.8 \cdot 10^4$	$2.0 \cdot 10^4$

TABLE I: Properties of the three CuAl6% closed membrane transducers. The transducers resonance frequencies has been estimated from the tuning procedure at room temperature as described in [14]

B. The calibrator

The calibrator is a capacitive resonant transducer. The impedance of the calibrator, biased with an electric field E_{cal} , for each mode of resonance ω_m , is given by

$$Z(\omega) = \frac{1}{i\omega C_{cal}} \left(1 - \frac{C_{cal} E_0^2}{m_m} \frac{1}{\omega_0^2 - \omega^2 + \frac{i\omega\omega_0}{Q_m}} \right) \quad (1)$$

The real part is used to estimate the energy of the mode and can be derived as follows

$$Re(Z(\omega)) = \frac{\omega_0 E_0^2}{m_m Q_m} \frac{1}{(\omega_0^2 - \omega^2)^2 + \frac{\omega^2 \omega_0^2}{Q_m^2}} = \frac{A_{m,0}}{(\omega_0^2 - \omega^2)^2 + \frac{\omega^2 \omega_0^2}{Q_m^2}} \quad (2)$$

on the calibrator method described here particularly interesting because it is free from systematic errors, at least to estimate the temperature of the mode.

C. The read-out system

Two transducers, named *transducer 1* and *transducer 2* were coupled respectively to the two-stage SQUID and to a single stage commercial Quantum Design SQUID. The third resonator, *transducer 3*, was coupled to a room temperature FET amplifier and was used for diagnostic and calibration purposes. Here we describe the performance of *transducer 1* coupled to a two-stage SQUID system based on a DROS [15],[16] as an amplifier and a Quantum Design dc SQUID as sensor SQUID. [14]. The complete read-out circuit of *transducer 1* is shown in figure 1.

The impedance matching between the transducer capacitance and the SQUID input coil is achieved by using a high-Q superconducting transformer. The electrical resonance of the transformer is not tuned to the mechanical modes, so the impedance matching is not optimal. The transformer coils were made of Nb wires and enclosed into a double superconducting shield. The bias circuit and the decoupling capacitor have been housed into a separate compartment of the superconducting shielding box. The measured transformer primary and secondary coil inductances are respectively $L_p = 0.3595 \pm 0.005 H$ and $L_s = 2.1 \pm 0.2 \mu H$. The mutual inductance between the coils was $M = (2.5 \pm 0.5) \cdot 10^{-5} H$ and the coupling factor $\alpha_{p,3} = 0.43$.

We use a decoupling Teflon commercial capacitor $C_d = 220 nF$ and SMD bias resistors for a total resistance of $R_{bias} = 13 G\Omega$ at $4.2 K$. The final intrinsic electrical quality factor, after connecting the decoupling capacitor C_d and the bias resistor R_{bias} , is equal to $Q = (1.8 \pm 0.1) \cdot 10^5$ at $4.2 K$.

The transducer has been assembled with a gap of about $20 \pm 2 \mu m$ and a capacitance $C = 1.17 \pm 0.01 nF$ measured at room temperature. This has been done in order to keep the electrical mode separated from the mechanical ones. The electrical mode resonance frequency measured on the antenna at $5 K$ was $8120 Hz$.

Two-stage SQUID systems are developed in order to reduce the noise of dc-SQUID amplifiers, which is normally limited by the room temperature electronics [15] [17] [18] [19]. When used in the transducer chain for resonant gravitational waves detectors, they can improve the detection sensitivity by orders of magnitude [8]. The system described here differs from other two-stage SQUIDS

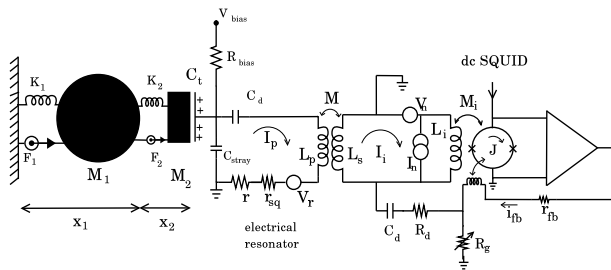


FIG. 1: Electro-mechanical scheme of a spherical antenna with mechanical resonator and capacitive transducer coupled to a SQUID through a superconducting matching transformer.

used in GW experiments since it uses a DROS as an amplifier SQUID [16]. A DROS has a large flux-to-voltage transfer function which allows direct read-out of the signal. Direct read-out simplifies multichannel read-out as needed in spherical gravitational wave detectors.

The two-stage SQUID system we developed is based on a configuration reported in [15, 20]. A standard dc-SQUID chip manufactured by Quantum Design (QD) [31] was chosen as sensor SQUID because of a larger input inductance with respect to the dc-SQUID described in [15].

The dc-SQUID is biased at a constant voltage by means of a resistor $R_{bias} = 1.5\Omega$. The current through the sensor SQUID is modulated by an applied signal flux Φ_{sig} and is fed through the input coil of the DROS. The total additive flux noise at 4.2 K is $\sqrt{S_{\Phi}} = 1.60 \pm 0.02 \mu\Phi_0/\sqrt{Hz}$ with input coil open and $\sqrt{S_{\Phi}} = 1.10 \pm 0.02 \mu\Phi_0/\sqrt{Hz}$ with input coil superconductively shorted. This corresponds respectively to an intrinsic uncoupled energy resolution of $\epsilon = S_{\Phi}/2L_{sq} = 650 \pm 15 \hbar$ and $\epsilon = 320 \pm 15 \hbar$. This is in agreement with the expected values calculated from the SQUID parameters using the standard model [9]. In order to avoid instability in the SQUID-resonator system we implemented a capacitive cold damping network in the feedback line. Damping network has been first investigated by Stevenson [21], using a phase-shifted inductive feedback, and by Vinante [8], who made use of a capacitive network. The two-stage SQUID coupled to a high quality factor electrical resonator showed the same performances [14]. We estimate at 4.2 K a SQUID noise temperature $T_N = 100 \pm 30 \mu K$ and a noise number $N = 730 \pm 100$. The additive coupled energy resolution was $650\hbar$ and $320\hbar$ respectively at 4.2 and 2.1 K.

III. EXPERIMENTAL RESULTS

A. Electrical system and noise spectrum

The additive noise level of the two-stage SQUID coupled to the transducer mounted on the sphere, was comparable with the one measured with the SQUID with

open input. When operating without the cold damping network, the minimum wideband flux noise observed with the SQUID was of $\sim 2.7 \mu\Phi_0/\sqrt{Hz}$. When the cold damping was active, we measured an additive wideband flux noise of $1.67 \pm 0.03 \mu\Phi_0/\sqrt{Hz}$. It corresponds to an additive coupled energy resolution of $730 \pm 100 \hbar$. As

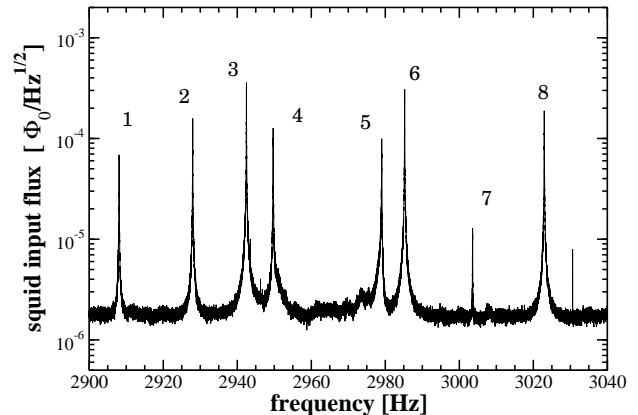


FIG. 2: Flux spectral density measured at the SQUID output with transducer bias at 200 Volt. All the expected 8 modes of the system are visible in the spectrum.

shown in figure 2, all the expected 8 modes of the system are visible in the spectrum. To establish which modes were strongly coupled to the transducer with the two-stage SQUID system, we proceeded as described in the next section.

B. Equivalent temperature of the coupled oscillators

The best and most direct way to estimate the noise of the system is to measure the input impedance of the transducer coupled to the read-out SQUID amplifier as described in [22, 23]. However, in this experimental test we did not implement in the matching transformer the necessary calibration coil. To estimate the temperature of the modes we can proceed as follows. The power spectral density at the output of the calibrator, when the back-action contribution of the room temperature amplifier is negligible, is

$$S_{V,CAL} = 4k_B T_{eq} Re(Z(\omega)), \quad (3)$$

where $Re(Z(\omega))$ was derived in Eqs. (1), T_{eq} is the equivalent temperature of the modes and we are considering monolateral spectra. At low temperature this value is too small to be measured with the room temperature FET amplifier. However, by exciting each modes at resonance with an auxiliary piezo-electric transducer (PZT), we can increase the signal at a level that can be measured by the FET amplifier. Then we read both the responses of the FET amplifier and the two-stage SQUID coupled to the resonator biased at a voltage $V_{b,sq}$. We assume that the

voltage $V_{CAL}(\omega)$ at the output of the FET is proportional to the voltage $V_{SQ}(\omega)$ at the output of the SQUID, i.e. $V_{CAL} = A_{cal,sq} V_{SQ}(\omega)$. This is true at resonance. If we now measure the power spectrum $S_{V,SQ}$ at the SQUID output, when the modes are not excited, we can evaluate the equivalent temperature of the modes using Eqs. (3), where we substitute

$$S_{V,CAL} = A_{cal,sq}^2 S_{V,SQ}. \quad (4)$$

Here we assumed that the system response is linear in the whole range. Linearity has been checked for different excitation voltage. We found a linear behaviour within 10%.

To estimate the equivalent temperature of the modes we measured the variance σ^2 of the stochastic process with a spectral noise $S_{V,SQ}$ at the output of the two-stage SQUID. From Eqs. (2), Eqs. (3) and Eqs. (4), defining $A_{m,0} = \frac{\omega_0 E_0^2}{m_m Q_m}$, the variance can be written as follows

$$\sigma_m^2 = \frac{4k_B T_{eq}}{2\pi} \frac{A_{m,0}}{A_{cal,sq}^2} \int_{(\omega_m - \Delta)}^{(\omega_m + \Delta)} \frac{d\omega}{(\omega_0^2 - \omega^2)^2 + \frac{\omega^2 \omega_m^2}{Q_m^2}}, \quad (5)$$

from where we obtain the relation which links the equivalent temperature of the mode to the variance of the stochastic process with spectral noise given by $S_{V,SQ}$. We have

$$T_{eq} = \frac{\omega_m^3 A_{cal,sq}^2}{2k_B A_{m,0} Q_m} \sigma_m^2 = \alpha_m \sigma_m^2, \quad (6)$$

where $A_{cal,sq}^2$ comes from the calibration as described in this section, and $A_{m,0}$ is estimated from the Lorentzian curve fitting of each resonance of the real part of the calibrator impedance.

To estimate σ_m a lock-in amplifier is used with the reference set at the resonance frequency of the mode. The lock-in amplifier output magnitude r and angular phase ϕ are then sampled at regular time intervals. The amplitude decay time constant of the lock-in amplifier is chosen equal to the sampling time $\tau_s = \tau_{lk}$. To observe the free evolution of the mode m the lock-in amplifier time constant is chosen smaller than the time constant of the mode, $\tau_{lk} < \tau_m$, but large enough that the lock-in amplifier works as a bandpass filter and makes the contribution of the broadband noise of the SQUID and the tails of the neighboring modes negligible. The mean square amplitude $\langle r^2 \rangle$ of the lock-in amplifier input signal magnitude, equal to the variance of the total narrow-band noise V_{nb}^2 , is given by [24]

$$\langle r^2 \rangle = V_{nb}^2 = \left(1 + \frac{\tau_{lk}}{\tau_m}\right) \left(\sigma_0^2 - \frac{S_{wb}}{2\tau_{lk}}\right), \quad (7)$$

where σ_0^2 is the variance of the power spectral density output, and S_{wb} is the power spectral density of the SQUID wideband noise. Generally the factor $\tau_m/(\tau_m + \tau_{lk}) \sim 1$ in our case.

The stochastic process r^2 is the sum of two independent Gaussian processes, the in-phase and quadrature lock-in amplifier output. If the signal is absent or in general if its average contribution is negligible with respect to the noise, the variable r^2 will have the exponential distribution $F(r^2) = \frac{1}{2\sigma_0^2} e^{-\frac{r^2}{2\sigma_0^2}}$.

The estimate of σ_0^2 , is then performed by sampling the magnitude r at regular time intervals, with sampling time $\tau_s \ll \tau_m$. A subset of data is created by extracting a data point every resonator time constant τ_m in order to get uncorrelated samples. After a large number of samples is collected, a histogram $N(r^2)$ is built, where N is the number of samples in a given bin around r^2 . The histogram is fit with the exponential distribution described above and the mean square amplitude $\langle r^2 \rangle$ is then extracted as fitting parameter.

In the absence of excess or amplifier back-action noise, the quantity $\langle r^2 \rangle$ is proportional to the thermal vibrational energy in the antenna mode. The constant of proportionality α_m was used to rescale the recorded values of $\langle r^2 \rangle$ to antenna energy. For the two most coupled modes at frequencies 2943 Hz and 2985 Hz we found the calibration factor α_m to be $\alpha_{2943} = (7.0 \pm 1.5) \cdot 10^8 [K/V^2]$ and $\alpha_{2985} = (1.1 \pm 0.2) \cdot 10^9 [K/V^2]$ respectively.

Graphs (a) and (b) in figure 3 show the energy distribution estimated for the modes at frequencies 2943 Hz and 2985 Hz during three hours of acquisition. The equivalent temperature for both modes is obtained by fitting the exponential distribution.

The slope of the distribution corresponds to a temperature of $7.0 \pm 2 K$ for the mode at 2943 Hz and $9 \pm 2 K$ for the mode at 2985 Hz, the error arising mainly from the calibration uncertainty. The equivalent temperatures are consistent, within two sigma, with the thermodynamic temperature of the sphere. No significant difference is observed in the equivalent temperature of the mode between night and day acquisitions.

C. Force calibration and strain sensitivity

When the mode m is excited at resonance ω_m with an energy given by $\frac{1}{2} k_B T_m$, the power spectral density measured at the SQUID output is

$$S_{v,sq} = \frac{4k_B T_m \text{Re}(Z(\omega_m))}{A_{cal,sq}^2} \left[\frac{V^2}{Hz} \right], \quad (8)$$

where $\text{Re}(Z(\omega))$ is the real part of the calibrator impedance.

The force power spectral density of a mode excited at a temperature T_m , when back action is negligible like in our case, is given by

$$S_{FF,m} = \frac{4k_B T_m m_{eff,m} \omega_m}{Q_m} \left[\frac{N^2}{Hz} \right], \quad (9)$$

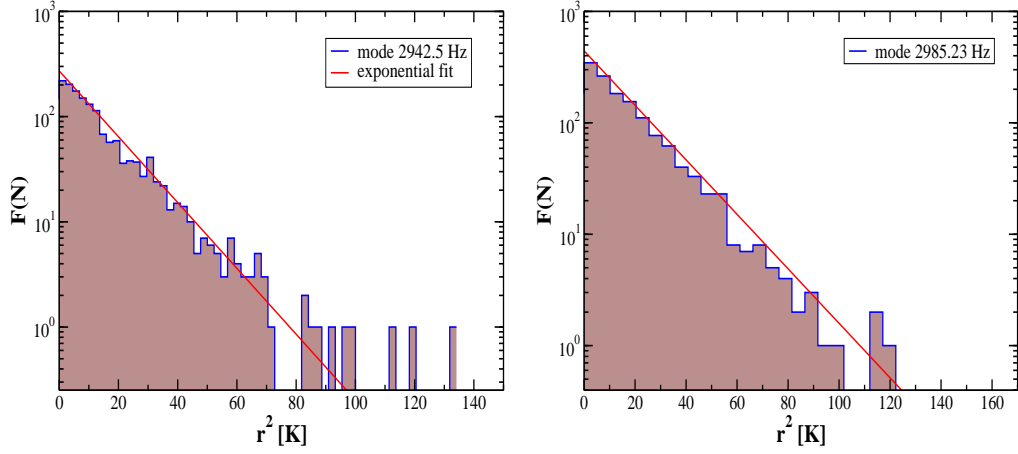


FIG. 3: Exponential distributions of the mean square amplitude $\langle r^2 \rangle$ for the modes at 2943 Hz and 2985 Hz. The variance σ_m^2 obtained from the fit of the exponential distribution gives an equivalent temperature of the two modes of $7.0 \pm 2 K$ and $9 \pm 2 K$ respectively

where $m_{eff,m}$ is the effective mass of the mode m , which can be estimated from the tuning curves of the sensor transducer if the bias voltage and the gap are known. [32] From the ratio of Eqs. (8) and Eqs. (9) we get

$$\frac{S_{v,sq}}{S_{FF,m}} = \frac{Q_m Re(Z(\omega))}{m_{eff,m} \omega_m A_{cal,sq}^2} \left[\frac{V^2}{N^2} \right]. \quad (10)$$

From the calibrator impedance measurement, we have

$$Re(Z(\omega)) = \frac{A_{m,c}}{(\omega_{m,c}^2 - \omega^2)^2 + \frac{\omega^2 \omega_{m,c}^2}{Q_{m,c}^2}} \quad (11)$$

where $\omega_{m,c}$ and $Q_{m,c}$ were measured during the calibration process and were different from the resonance measured during the acquisition of the mode spectra because, in the later case, the calibrator was not charged. $A_{m,c}$ is obtained from the Lorentzian fit of each mode of the real part of the calibrator impedance.

At each mode resonance Eqs. (10) becomes

$$\left(\frac{S_{v,sq}}{S_{FF,m}} \right)_{\omega=\omega_m} = \frac{Q_m A_{m,c}}{m_{eff,m} \omega_m A_{cal,sq}^2} \frac{Q_{m,c}^2}{\omega_m^4} \left[\frac{V^2}{N^2} \right]. \quad (12)$$

We now turn to analyze the detector transfer functions. The relations derived so far are valid at resonance. As a first approximation, one can consider the transfer function $\mathcal{G}_{SQ,F}$ as a product of poles and zeros where the poles are derived from the polynomial fit of the SQUID noise spectrum and the zeros are chosen to fit the measured amplitude at resonance given by Eqs. (12).

The transfer functions for an applied calibration signal becomes

$$\mathcal{G}_{SQ,F}(\omega) = H_{m,cal}(\omega) \frac{\prod_{k=1}^{N_r} (j\omega - r_{k,m})(j\omega - r_{k,m}^*)}{\prod_{k=1}^{N_p} (j\omega - p_k)(j\omega - p_k^*)}. \quad (13)$$

In the equation above $N_p > N_r$ and $H_{m,cal}(\omega)$ is a force calibration constant which has been experimentally determined from the calibration measurement at resonance.

All the terms included in Eqs. (12) and Eqs. (13) are derived experimentally from the calibration, from the tuning curves and from direct measurement of the modes quality factor. The transfer function is experimentally measured at resonance and only approximated out of resonance.

We remark again that quality factors and resonance frequencies are different when measured during calibration ($\omega_{m,c}$, $Q_{m,c}$) and during acquisition of the noise spectra ($\omega_{m,s}$, $Q_{m,s}$), due to the bias voltage in the calibrator. This complication arises from the fact that the calibrator was also coupled to the quadrupolar modes of the sphere. This effect is included in the estimate transfer function of Eqs. (13).

A small parenthesis needs to be opened here. While for a bar detector it is relatively straight forward to relate the strain produced by a calibrator located on one of the bar faces with the strain from a gravitational wave signal, the same cannot be said for a spherical detector. A calibration *hammer stroke* excites a linear combination of the five spheroidal modes depending on the position on the sphere surface. When only one calibrator is used, like for the Minigrail test run described in this paper, one only calibrates the detector for a particular set of forces \mathbf{F}_m applied to each spheroidal mode. Such a combination of forces might not always represent a GW excitation. In order to fully calibrate the detector one needs to generate calibration forces from a set of 5 or more calibrators located at different positions on the sphere surfaces. A detailed procedure to calibrate a spherical detector is described in [23].

In the experiment described here, the calibration signal is generated by a piezo located at position ($\theta = 18^\circ$, $\phi = 135^\circ$). By using Eq. 45 in [23], derived previously in [3, 5, 25], one finds that a piezo in such a location excites

a combination of the 5 spheroidal modes given by the vector $(0, 0.13, -0.49, 0.5, -1)$, normalised to the maximum value of its elements. One can see that such a combination is equal, within 20% tolerance, to the one generated by a circularly polarised gravitational wave coming from direction $(\theta = 20^\circ, \phi = 135^\circ)$. Following [23] one can see that such a wave direction is almost optimal for a transducer configuration described in this paper.

MiniGRAIL strain sensitivity with three transducers coupled to the spheroidal modes, but only one used for the read-out, is shown in figure 4. The read-out transducer was biased with a constant electric field of $E = 10^7 \text{ Volt/m}$ and the sphere thermodynamic temperature was 5.2 K . As discussed above, the experimental strain curve gives an estimation of the detector sensitivity only for a particular combination of spheroidal modes corresponding to a gravitational wave coming from the $(\theta = 20^\circ, \phi = 135^\circ)$ direction.

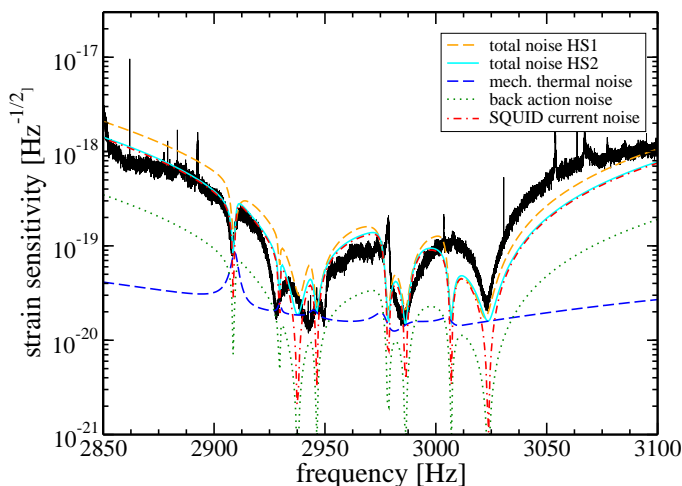


FIG. 4: MiniGRAIL strain sensitivity at 5 K with three transducer placed on the sphere, but single transducer read-out. The sensitivity has been estimated for a particular combination of the 5 spheroidal modes as derived by exciting the mode using a piezo transducer (PZT) located at $(\theta = 18^\circ, \phi = 135^\circ)$. The dashed gray curve shows the strain sensitivity calculated for a simulated hammer stroke excitation from the PZT location using the electro-mechanical model described in [23]. For the simulation we used the detector parameters discussed here in the text. A better matching between the experimental data and the simulation is obtained when the simulated hammer stroke is given at the position $(\theta = 27^\circ, \phi = 135^\circ)$ (continuous gray curve). The other curves show the contribution of the thermal noise (dashed dark line) and the back-action noise (dotted line) to the strain sensitivity.

We obtained a peak strain sensitivity of $(1.5 \pm 0.6) \cdot 10^{-20} \text{ Hz}^{-1/2}$ at 2942.9 Hz and a strain sensitivity of about $5 \cdot 10^{-20} \text{ Hz}^{-1/2}$ over a bandwidth of 30 Hz . This corresponds to a strain amplitude of $h \simeq 2.5 \cdot 10^{-18}$ at 3 kHz for a burst signal of 1 ms [26]. For a sphere of 68 cm in diameter like the one of MiniGRAIL, it is equivalent to a displacement sensitivity, at 3 kHz , of

$1.6 \cdot 10^{-19} \text{ m}$. When optimal filtering is applied to the output signal, the detector is sensitive to burst signals with an impulse energy of about $T_N \sim 50 \text{ mK}$ as can be derived calculating the noise temperature using the experimental data. This sensitivity would be enough to detect supernova explosions in our galaxy. The calculated sensitivity curves in figure 4, are obtained using the model described in [23]. The dashed gray curve shows the strain sensitivity calculated for a simulated hammer-stroke excitation applied to the same point on the sphere where the PZT is placed, i.e. $(\theta = 18^\circ, \phi = 135^\circ)$. The simulated signal describes reasonably well the strain sensitivity.

The best fitting strain sensitivity has been obtained for a simulated hammer stroke applied at the sphere surface point $(\theta = 27^\circ, \phi = 135^\circ)$. The result is shown with the continuous gray line. In this case the third mode is more excited. The agreement with the experimental data is rather impressive considering the amount of fitting parameters involved in the simulation. The difference of about 7° in the angle θ of the experimental and simulated excitation position could be explained considering the fact that a spherical detector with only three transducers in the position 1, 2 and 5 like the one considered here is far from being symmetric. In [27] the authors had to perform a rotation of spheroidal mode reference frame as well to be able to explain their experimental results. In their case the transducers were not as massive as here and, above all, they used six transducers positioned in the symmetric TI configuration. The resulting mixing of the spheroidal modes could explain the discrepancy between the measured and the simulated sensitivity curves. In order to address more accurately this issue one should place on the sphere at least 5 calibrators to measure the detector response to each of the 5 spheroidal modes. When six transducer are fully operating with comparable sensitivity, a single calibrator is enough to fully calibrate the detector as shown in [23, 27].

The contribution to the strain sensitivity of the well known noise sources are plotted in figure 4 as well. At resonance, the sensitivity is limited by mechanical thermal noise of the transducer mass. Out of resonance the sensitivity is limited by the SQUID additive current noise. The back action noise of the SQUID is about an order of magnitude smaller. The electrical thermal noise of the superconducting transformer, not shown in the graph, is negligible because the electrical mode is well decoupled from the mechanical ones.

From the measurement of the variance of the most coupled modes and the simulated data we can conclude that, within the experimental accuracy, the MiniGRAIL peak sensitivity is currently limited by the thermal noise generated by the transducer mass. Some of the modes, however, show excess noise whose origin is difficult to address. A better estimate of the transfer function of each spheroidal mode is necessary in order to fully characterise the detector. The measurements presented here have to be considered as a first test bed for the following engi-

neering and science runs of Minigrail. The sensitivity is expected to improve of at least one order of magnitude when the detector will operate at 20 mK.

In figure 5 the measured strain sensitivity is shown together with predicted sensitivity for possible future detector configurations. A polynomial fit of the strain sensitivity is shown as well. The poles and zeros obtained from the fit can be used to build the matched filters for GW detection [23]. The expected strain sensitivity of Minigrail is shown for the detector operating at $T = 50 \text{ mK}$ with the same three transducers configuration presented here. The figure shows the expected sensitivity for a Minigrail II. In this configuration Minigrail operates with 6 capacitive transducers placed in the TI configuration where the electrical modes are coupled to the mechanical ones. We consider $T/Q = 2.5 \times 10^{-8} \text{ K}$ and a SQUID coupled energy resolution $E_{\text{coupled}} = 70\hbar$. Those values are achievable within the current technology. See [23] for a recent review. The sensitivity of Minigrail operating at the quantum limit is also shown. Minigrail can reach a peak sensitivity of about $6 \cdot 10^{-23} \text{ Hz}^{-1/2}$ and a bandwidth larger than 400 Hz at a sensitivity of $1 \cdot 10^{-22} \text{ Hz}^{-1/2}$.

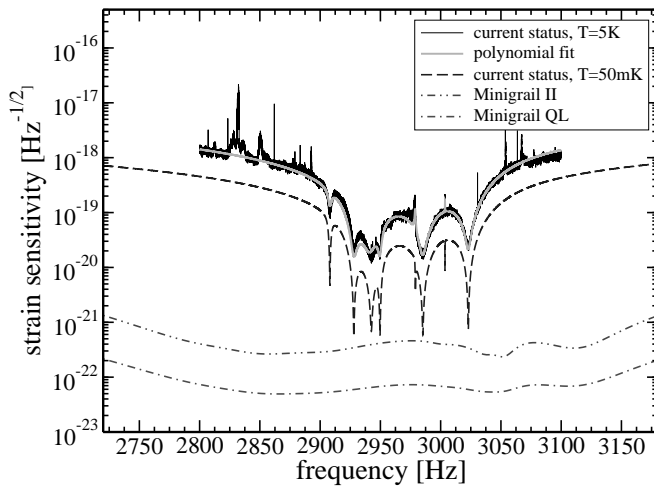


FIG. 5: The measured strain sensitivity of MiniGRAIL is shown together with predicted sensitivity for future detector configurations. The continuous gray line is a polynomial fit of the measured strain sensitivity. The dashed line shows the sensitivity for the detector operating at $T = 50 \text{ mK}$ with the same three transducers configuration presented in this paper. The dot-dot-dashed line (Minigrail II) shows the sensitivity achievable with available technology, namely $T/Q \sim 2.5 \times 10^{-8} \text{ K}$ and SQUID energy resolution $E = 70\hbar$. The dot-dashed curve gives the sensitivity for a quantum limited detector (Minigrail QL) with $T/Q \sim 1 \times 10^{-9} \text{ K}$.

IV. CONCLUSIONS

We have operated at 5 K a spherical resonant detector equipped with a capacitive resonant transducers coupled to a two-stage SQUID amplifier. Our two-stage SQUID amplifier is one of the most sensitive amplifier employed so far on a GWs resonant detector. We measured an additive coupled energy resolution of $700 \pm 100 \hbar$ at 5K. We reach a peak strain sensitivity of $1.5 \cdot 10^{-20} \text{ Hz}^{-1/2}$ at 2942.9 Hz. A strain sensitivity of better than $5 \cdot 10^{-20} \text{ Hz}^{-1/2}$ has been obtained over a bandwidth of 30 Hz. We expect an improvement of more than one order of magnitude when the detector will operate at 50mK. This result should be considered as the first step towards the realization of an ultracryogenic spherical gravitational wave detector.

Acknowledgments

The authors would like to acknowledge precious discussions with Jean-Pierre Zendri, Paolo Falferi, Andrea Vinante and Alberto Lobo. We are grateful to Hibbe van der Mark for his technical help. This work has been partially financially supported by Integrated Large Infrastructures for Astroparticle Science (ILIAS) of the Sixth Framework Programme of the European Community.

....

-
- [1] E. Coccia, J. A. Lobo, and J. A. Ortega, Phys. Rev. D **52**, 3735 (1995).
 - [2] J. A. Lobo, Phys. Rev. D **52**, 591 (1995).

- [3] S. M. Merkowitz, Phys. Rev. D **58**, 062002 (1998).
- [4] C. Z. Zhou and P. F. Michelson, Phys. Rev. D **51**, 2517 (1995).

- [5] T. R. Stevenson, Phys. Rev. D **56**, 564 (1997).
- [6] A. de Waard, M. Bassan, Y. Benzaim, V. Fafone, J. Flokstra, G. Frossati, L. Gottardi, C. T. Herbschleb, A. Karbalai-Sadegh, K. Kuit, et al., Classical and Quantum Gravity **23**, S79 (2006).
- [7] O. D. Aguiar, L. A. Andrade, J. J. Barroso, F. Bortoli, L. A. Carneiro, P. J. Castro, C. A. Costa, K. M. F. Costa, J. C. N. de Araujo, A. U. de Lucena, et al., Classical and Quantum Gravity **23**, S239 (2006).
- [8] A. Vinante, M. Bonaldi, P. Falferi, M. Cerdonio, R. Mezzena, G. Prodi, and S. Vitale, proceedings of the "SQUID 2001 Conference", Sept. 1-3, 2001, Stenungsbaden, Sweden, Physica C **368**, 176 (2002).
- [9] C. D. Tesche and J. Clarke, *J. Low Temp. Phys.* **29**, 301 (1977).
- [10] A. de Waard, L. Gottardi, M. Bassan, E. Coccia, V. Fafone, J. Flokstra, A. Karbalai-Sadegh, Y. Minenkov, A. Moleti, G. V. Pallottino, et al., Classical and Quantum Gravity **21**, S465 (2004).
- [11] P. Falferi, M. Bonaldi, M. Cerdonio, A. Vinante, R. Mezzena, and G. P. adn S. Vitale, Appl. Phys. Lett. **88**, 062505 (2006).
- [12] M. Podt and L. G. and, Phys. Rev. D **65**, 0420041 (2004).
- [13] A. de Waard, Y. Benzaim, G. Frossati, L. Gottardi, H. van der Mark, J. Flokstra, M. Podt, M. Bassan, Y. Minenkov, A. Moleti, et al., Classical and Quantum Gravity **22**, S215 (2005).
- [14] L. Gottardi, Ph.D. thesis, Leiden University, Leiden, The Netherlands (2004).
- [15] M. Podt, M. J. van Duuren, A. W. Hamster, J. Flokstra, and H. Rogalla, Appl. Phys. Lett. **75**, 2316 (1999).
- [16] M. J. van Duuren, G. C. S. Brons, J. D. J. Adelerhof, and H. Rogalla, J. Appl. Phys. **82**, 3598 (1997).
- [17] R. Mezzena, A. Vinante, P. Falferi, S. Vitale, M. Bonaldi, G. A. Prodi, M. Cerdonio, and M. B. Simmonds, Rev. Sci. Instrum. **72**, 3694 (2001).
- [18] G. M. Harry, J. Houser, and K. A. Strain, Phys. Rev. D **65**, 082001 (2002).
- [19] P. Carelli, M. G. Castellano, G. Torrioli, and R. Leoni, Appl. Phys. Lett. **72**, 115 (1998).
- [20] L. Gottardi, M. Podt, M. Bassan, J. Flokstra, A. Karbalai-Sadegh, Y. Minenkov, W. Reinke, A. Shumack, S. Srinivas, A. de Waard, et al., Classical and Quantum Gravity **21**, S1191 (2004), URL <http://stacks.iop.org/0264-9381/21/S1191>.
- [21] T. R. Stevenson and H. J. Haucke, in *Proc. of the 1st Edoardo Amaldi Conf. on Gravitational Waves* (World Scientific, Singapore, 1995), p. 390.
- [22] L. Baggio, M. Bignotto, M. Bonaldi, M. Cerdonio, L. Conti, P. Falferi, N. Liguori, A. Marin, R. Mezzena, A. Ortolan, et al., Phys. Rev. Lett. **94**, 241101 (2005).
- [23] L. Gottardi, Phys. Rev. D **75**, 022002 (2007).
- [24] P. Bonifazi, V. Ferrari, S. Frasca, G. V. Pallottino, and G. Pizzella, *Il Nuovo Cimento* **1C-6**, 465 (1978).
- [25] J. A. Lobo, Mon. Not. Roy. Astr. Soc. **316**, 173 (2000).
- [26] E. Coccia (World Scientific, Singapore, 1996), Proc. of the International Conference on Gravitational Waves: Sources and Detectors, p. 201.
- [27] S. M. Merkowitz and W. W. Johnson, Phys. Rev. D **56**, 7513 (1997).
- [28] H. J. Paik, J. Appl. Phys. **47**, 1168 (1976).
- [29] J. P. Richard, Phys. Rev. Lett. **52**, 165 (1984).
- [30] Y. Ogawa and P. Rapagnani, Nuovo Cimento **7C**, 21 (1984).
- [31] Quantum Design, 11578 Sorrento Valley Road, San Diego
- [32] In a capacitive transducer the bias electric field introduces a negative spring constant which causes the resonant frequency of the transducer resonator to shift down. In the simplest case, this shifted frequency is related to the transducers electro-mechanical coupling coefficient β by $\beta = -\frac{\omega_t^2 - \omega_0^2}{\omega_t^2}$ [28]. β is defined as the ratio between the mechanical and the electrical energy, and describes the conversion efficiency of mechanical motion into electrical signal. It can be written as follows [29] $\beta = \frac{1}{d_0^2} \frac{C_t V^2}{\omega^2 m_{eff}}$ where the effective mass m_{eff} includes possible geometrical factors [30] as well as electrical parameters from the coupled circuit. See [14] for more details on the tuning procedure.